RESEARCH ARTICLE

The Network Ontogeny of the Parrot: Altriciality, Dynamic Skeletal Assemblages, and the Avian Body Plan

Julieta Carril[1] · Claudia P. Tambussi[2] · Diego Rasskin-Gutman[3]

Abstract

We analyze the connectivity patterns and fusion events among bones leading to the adult skeletal organization during the development of the superaltricial monk parakeet (*Myiopsitta monachus*, Psittaciformes), providing insights about the functional and evolutionary significance in the avian structural design. By using whole mount specimens stained for cartilage and bone, we apply anatomical network analysis (AnNA) to study the ontogenetic trajectory of the entire skeleton from embryonic stage 34 to adult. As bones condense, connect, and fuse to each other, we follow skeletal assemblages forming networks that change dynamically as the monk parakeet grows. Our results show that the pelvic girdle connects with the vertebral column prior to the pectoral girdle and that the pelvic girdle and hindlimbs connection begins and ends before that of the pectoral girdle and the forelimbs. We hypothesize that connections of the girdles and limbs could be linked to the altriciality of the species due to requirements for active movement in the use of the hindlimbs inside the nest, but not the need to use forelimbs to fly until much later. Further, as bones of the skull and pelvis fuse during development they form the largest and more connected assemblages, acting as attractors to connect to other bones, showing congruence between the connectivity pattern at each ontogenetic stage and the characteristic avian body plan.

Introduction

Despite a multitude of differing ways of life, whether flying or flightless, there is a body plan that unequivocally groups all birds and segregates them from the rest of the vertebrates.

✉ Julieta Carril
  julyetacarril@gmail.com

1 Laboratorio de Histología y Embriología Descriptiva, Experimental y Comparada (LHYEDEC), Facultad de Ciencias Veterinarias, Universidad Nacional de La Plata, Consejo Nacional de Investigaciones Científicas y Técnicas (CONICET), Buenos Aires, Argentina

2 Centro de Investigaciones en Ciencias de La Tierra (CICTERRA), Universidad Nacional de Córdoba, Consejo Nacional de Investigaciones Científicas y Técnicas (CONICET), Córdoba, Argentina

3 Grupo de Investigación en Biología Teórica, Instituto Cavanilles de Biodiversidad y Biología Evolutiva, Universidad de Valencia, Valencia, España

Major structural features that characterize the avian body plan (bauplan) are present at the skeleton level, with a reorganization of both limbs and a general simplification due to loss or fusion of bones. Interestingly, these derived features were already present in the basal nodes of the avian crown group (latest Cretaceous or earliest Palaeogene) (Clarke et al. 2005; Lee et al. 2014).

An important parameter in avian evolution is the degree of development of the offspring at hatching, which leads to different postnatal growth rates and different scaling of body parts in relative terms (i.e. allometry) (Starck 1993). To understand how internal constraints limit structural changes and how different environments (external selective forces) guide the evolution of avian ontogenies, it is necessary to obtain developmental data using a multitude of complementary approaches.

The terms precocial and altricial refer to the degree of behavioral and morphological maturation of the offspring at hatching. It is well known that different developmental trajectories influence morphology, physiology, ecology and behavior, and are key to understanding many aspects of the lifestyle and abilities of different avian species (Starck 1993).

The extreme modes of development in the altricial-precocial spectrum extend from superprecociality, where the offspring resemble adult birds and are completely independent after hatching, to superaltriciality (altricial 2 sensu Starck 1993), where the offspring resemble an embryo-like state and their dependence of parental care at hatching is total (Ricklefs and Starck 1998). Despite this, and the fact that birds are the most speciose group of land vertebrates (Prum et al. 2015), knowledge of avian skeletal development, especially of non-model altricial species, is still very limited.

The development of the superaltricial monk parakeet *Myiopsitta monachus*, a Neotropical psittaciform, has been previously studied from different perspectives by our research team, including its complete ossification sequence and the recognition of sequence heterochronies within birds (Carril and Tambussi 2017). Here we approach the skeletogenesis of this species using anatomical network analysis (AnNA) as a conceptual and methodological framework, which allows switching the focus of analysis to the connectivity patterns that arise as the skeleton grows. Thus, the aim of this work is to provide new insights regarding the sequence of bone to bone connection and fusion events leading to the adult skeletal organization during the development of the monk parakeet, as well as its functional and evolutionary significance in the avian structural design.

AnNA is a novel, powerful, quantitative, and accessible approach that have been developed in the past 10 years to investigate morphological information at the level of connectivity among anatomical parts like bones, cartilage, tendons or muscles (Rasskin-Gutman and Esteve-Altava 2014). As such, it supplies new information that complements classic morphological analytical tools (e.g., traditional geometric morphometrics). Using connectivity data, AnNA allows investigating the physical relation among whole anatomical elements; in other words, it treats an anatomical unit as a system of connected elements, offering a conceptual means of understanding their mutual influence. Evolutionary, developmental and evolutionary-developmental (Evo-Devo) insights can be inferred using this tool once the properties of the networks are properly analyzed, particularly as a direct quantification of the notion of developmental burden (see AnNA as an Evo-Devo tool, Esteve-Altava and Rasskin Gutman 2018; Rasskin-Gutman and Esteve-Altava 2018). The notion of burden, originally from Riedl (1978), is part of the broader idea of developmental constraint based on von Baer's developmental laws. It states that the more connected an element during embryonic development is, the more functional dependencies it will have, constraining its future opportunities to change (Schoch 2010; Rasskin-Gutman and Esteve-Altava 2018).

Most published work with AnNA has focused on the human skull; for example, structural modularity (Esteve-Altava et al. 2013a, 2015), growth models (Esteve-Altava

and Rasskin-Gutman 2014a), or the relationship between development, evolution and pathological synostosis (Esteve-Altava and Rasskin-Gutman 2015; Esteve-Altava et al. 2017). However, due to its coarse-grained usability, AnNA can be applied in broad anatomically and phylogenetic contexts; for example, the evolutionary loss and fusion of bones in the tetrapod skull (Esteve-Altava et al. 2013b, 2014), phylogenetic comparative analysis of the complexity of the tetrapod skull (Esteve-Altava and Rasskin-Gutman 2014b), or the evolutionary and developmental dependencies of the origin of the mammalian middle ear (Navarro-Diaz et al. 2019). Although, as noted, AnNA has been used in many anatomical contexts, no studies primarily focusing on avian development have so far been undertaken, but see, Plateau and Foth (2020) for a recent AnNA study on peramorphosis of the bird skull. In addition, our study is also the first to apply this tool to include the entire bird skeleton.

The current work is focused on two guiding questions: (1) are there any patterns (in manner, time and/or rates) in the connections and fusions of bones during development that correlate with altriciality? and (2) which connections and fusions of bones occurring during development could be associated with morphological changes linked to the avian body plan? To address these questions, we have traced the sequence of connections and fusions between all bones of the monk parakeet skeleton.

Materials and Methods

We used a total of 36 specimens of the monk parakeet *Myiopsitta monachus* housed in our collection (Laboratorio de Histología y Embriología Descriptiva, Experimental y Comparada, Facultad de Ciencias Veterinarias, Universidad Nacional de La Plata, Buenos Aires, Argentina) (Supplementary Table 1). Specimens of this pest species (Canavelli et al. 2013) were obtained from nests during breeding seasons (from October to February, Collar 1997) in Córdoba province, Argentina. They were sacrificed following the protocols approved by the animal care committee and adhering to the legal requirements of Argentina, fixed in a 10% formalin solution for 48 h and preserved in 70% alcohol.

The assignment of embryonic stages (34 to 40+) was performed based on the external morphological descriptions of Carril and Tambussi (2015) and the nestling ages (samples available from newly hatched to 22 days old) were calculated using the equation of the length of the digit III of the hindlimb proposed by Aramburú (1997) (Supplementary Table 1).

In order to visualize and identify the bones (nodes) and their connections (physical junctions) we used a technique that differentially stain cartilages with alcian blue and bones with alizarin red, and digests the soft tissues with

the enzyme trypsin (Dingerkus and Uhler 1977). We have register ossification when bones show alizarin red staining (unlike Carril and Tambussi 2017). The osteological nomenclature follows Baumel and Witmer (1993).

For building networks, the topological information on bone-to-bone relationships was coded in adjacency matrices (i.e. symmetric binary matrices of size NxN, where 1 indicates presence and 0 indicates absence of connection) for the skeleton and throughout the ontogenetic trajectory of the monk parakeet, from embryonic stage 34 to adult (Supplementary Material 1). We assume that when a connection/fusion is observed at a stage/age, it occurs at that stage/age.

In AnNA, the nodes represent the anatomical elements and the links that connect them represent the structural relations or interactions among them. In this study, nodes are defined as the bones of the entire skeleton of the monk parakeet, and the links the physical junctions among them (i.e. tendinous and ligamentous junctions). All network parameters were obtained using R (R Core Team 2019), with package igraph (Csardi and Nepusz 2006). The following is a brief description of each parameter (see for more details Rasskin-Gutman and Esteve-Altava 2014), as well as for the new descriptor defined here as Dynamic Skeletal Assemblage (DSA). *Number of nodes (N):* simple count of nodes (bone condensation) at each stage. As growth proceeds, some nodes fuse, others disappear, and new names are assigned. *Number of interactions (K):* at each stage, we compute the total number of connections among bones. *Connectivity (degree, k_i):* the sum of connections that a specific node has to other nodes in the network at each stage. *Density of connections (D):* defined as the ratio of the number of interactions (K) and the total number of possible connections. *Mean shortest path length (L):* this average measures how close nodes are in terms of their connectivity. *Mean cluster coefficient (C):* this average is a measure of how triangulated is the system. *Heterogeneity (H):* this is a measure of how regular the system is in terms of individual number of connections for each bone. *Dynamic Skeletal Assemblages (DSAs):* we define here a DSA as a group of two or more connected nodes; these groups change at each stage as bones fuse or new bones connect to a particular assemblage. DSAs directly capture how the system groups from stage/age to stage/age until forming the connected adult.

Results

Bone Connections During Skeletogenesis (Tables 1 and 2, Figs. 1 and 2, Supplementary Material 2).

In the adult, 169 connections were identified between a total of the 132 bones analyzed. About 12% of them are established in ovo. These include connections between bones of

the dorso-lateral portion of the skull (squamosal, parietal, frontal and lacrimal), bones of the maxilla and palate (premaxillary, maxillary, palatine and pterygoid), bones of the jugal bar (jugal and quadratojugal) and maxilla, and the metatarsals (II, III and IV).

On the sixth day after hatching the connection of the skull with the vertebral column occurs. More precisely, this is evidenced because supraoccipital and exoccipital (not fused) connect with the cervical vertebra 1 (atlas).

At the vertebral column, the first vertebrae to connect are thoracic 1–5 at day 1.5, followed by the synsacral 1–12

Table 1 List of bones (nodes) sorted according to anatomical region, indicating their abbreviations (in Fig. 1, Table 2 and Supplementary Materials 1 and 2), and the fusions (in red) during the development of *Myiopsitta monachus*

Ossa cranii	
Os basioccipitale	bas
Os exoccipitale	exo
Os supraoccipitale	sup
Os parasphenoidale	pasp
Os laterosphenoidale	lat
Os squamosum	squ
Os parietale	par
Os frontale	fro
Os lacrimale	lac
Os ectecthmoidale	ect
Os mesethmoidale	mes
Os nasale (caudal)	nas(c)
Os premaxillare (caudal)	pre(c)
Os squamosum + Os parietale	sqpa
Ossa cranii 1 (bas+exo+sup+pasp)	cran1
Ossa cranii 2 (lat+squ+par+fro+lac+ect+mes)	cran2
Ossa cranii (Ossa cranii 1+Ossa cranii 2+nas(c)+pre(c))	cran
Ossa Maxillae et palati	
Os nasale (rostral)	nas(r)
Os premaxillare (rostral)	pre(r)
Os maxillare (corpus)	maxc
Os maxillare (proc. jugalis)	maxj
Os palatinum	pal
Os pterygoideum	pte
Os jugale	jug
Os quadratojugale	quaj
Os quadratum	qua
Ossa maxillae (nas(r)+pre(r)+maxc+pal)	maxil
Arcus jugalis (maxj+jug+quaj)	arj
Ossa mandibulae	**mand**
Os dentale	
Os supra-angulare	
Os angulare	
Os spleniale	
Os prearticulare	
Os articulare	art
Apparatus hyobranchialis	
Paraglossal	pg
Basihyale	bahy
Urohyale	uroh
Ceratobranchiale	cer
Epibranchiale	epb
Paraglussum (pg left+rigth)	par
Basihyale-Urohyale	baur

Table 1 (continued)

Columna vertebralis	
Vertebrae cervicales 1-14	vce1-14
Vertebrae thoracicae 1-5	vth1-5
Vertebrae synsacrales 1-12	vsy1-12
Vertebrae caudales 1-7	vca1-7
Costa incompletae 1-2	cin1-2
Costa completae verae (vertebralis) 1-5	cvv1-5
Costa completae verae (sternalis) 1-5	cvs1-5
Costa completae spuriae (vertebralis) 1	csv1
Costa completae spuriae (costalis) 1	csc1
Processus uncinatus (cin2)	pci
Processus uncinatus (cvv1-4)	pcv1-4
Pygostilus (vca6+vca7)	pyg

Ossa cinguli membri thoracici	
Sternum	ster
Scapula	sca
Os coracoideum	cor
Clavicula	clav
Furcula (clav left+right)	fur

Ossa membri thoracici	
Humerus	hum
Radius	rad
Ulna	uln
Os carp radiale	crad
Os carpi ulnare	culn
Os metacarpale alulare (II)	mca
Os metacarpale majus (III)	mcma
Os metacarpale minus (IV)	mcmi
Phalanx digiti alulae	pda
Phlanx proximalis digiti majoris	ppdm
Phlnx distalis digiti majoris	pddml
Phalanx digiti minoris	pdmi
Capometacarpus (mca+mcma+mcmi)	cmc

Ossa cinguli membri pelvici	
Ilium	ili
Ischium	isch
Pubis	pub
vsy1-4+ili	pelv1
vsy1-6+ili	pelv2
vsy1-9+ili	pelv3
vsy1-9+ili+isch+pub	pelv4
Pelvis (vsy1-12+ili+isch+pub)	pelv

Ossa membri pelvici	
Femur	fem
Tibiotarsus	tbt
Fibula	fib
Os metatarsale I-IV	mt1-4
Digit I Phalanx I-ungualis	d1p1-u
Digit II Phalanx I-ungualis	d2p1-u
Digit III Phalanx I-ungualis	d3p1-u
Digit IV Phalanx I-ungualis	d4p1-u
Os metatarsale II + Os metatarsale III	mt23
Tarsometatarsus (mt2+mt3+mt4)	tmt

at day 2.5, the cervical 1–14 at day 3, and finally the caudal 1–7 at day 15.

Ilium and synsacral vertebrae 1–4 connect at day 0, while the sternum and sternal ribs 1–5 connect after day 22 (and through them with the vertebrae). From this moment, both girdles are linked with the vertebral column.

In the pectoral girdle, the scapula connects with the coracoid at day 9, the coracoid with the furcula (fused clavicles) at day 12, and the coracoid and furcula with the sternum after day 22.

In the pelvic girdle, the ischium connects with the pubis at day 0.5, and the synsacral vertebrae + ilium connects with both ischium and pubis at day 12.

In the forelimbs, the humerus connects with the scapula and coracoid at day 22. The remaining connections of forelimbs occur after day 22.

Finally, in the hindlimbs, the metatarsals II-IV connect at embryological stage 36, and the femur connects with the pelvic girdle (synsacral vertebrae 1–9 + ilium and ischium + pubis) at day 18. The remaining connections of hindlimbs also occur at day 18.

Bone Fusions During Skeletogenesis (Tables 1 and 2, Figs. 1 and 2, Supplementary Material 2).

Four of the seven pairs of the elements of the mandible are the first to fuse in the entire skeleton at stage 36 (dental + supra-angular + angular + splenial). The pair of prearticular bones fused to each hemimandible at stage 38, hemimandibles fuse together at stage 40 +, and the articular bones are the last ones to fuse and complete the mandible at day 22.

In the skull, the squamosal and parietal bones fuse first at day 0.5 followed by the basioccipital + exoccipital + supraoccipital + parasphenoidal at day 15, and the laterosphenoidal + squamosal + parietal + frontal + lacrimal + ectethmoidal + mesethmoidal at day 22. All these elements fuse together in the adult.

In the maxilla, the pair of premaxillary bones fuses together at stage 40, then they fuse with the maxillary (corpus) at day 15, and finally with the palatine and nasal bones at day 18.

In the pectoral girdle, the clavicles fuse at stage 38 making up the furcula.

In the pelvic girdle, fusion of the synsacral vertebrae 1 to 4 and the ilia bones occur at day 9. The remaining synsacral vertebrae fuse in an antero-posterior direction (synsacral vertebrae 5 and 6 at day 12, 7 to 9 at day 15, and 10 to 12 in the adult), and the ischium and pubis bones fuse to the ilium at day 22. As a result, in the adult the pelvis is composed by the fusion of the synsacrum (synsacral

Table 2 Dynamic Skeletal Assemblages (DSAs) and fusions (in red) during the development of *Myiopsitta monachus*

	Ossa Mandibulae	Ossa cranii	Ossa Maxillae et palati	Columna vertebralis	Ossa cinguli membri pelvici	Ossa membri pelvici	Ossa cinguli membri thoracici	Ossa membri thoracici	Appartus hyobranchialis
S34	–	–	–	–	–	–	–	–	–
S36	mandl-mandr	–	–	–	–	mt2-mt3-mt4	–	–	–
S38	mandl-mandr	–	pal-pte / max-jug-quaj	–	–	mt2-mt3-mt4	–	–	–
S40	mandl-mandr	–	pre-pal-pte-max-jug-quaj	–	–	mt2-mt3-mt4	–	–	–
S40+	mand	lac-fro-par-squ	pre-pal-pte-max-jug-quaj	–	–	mt2-mt3-mt4	–	–	–
D0	mand	lac-fro-par-squ	pre-pal-pte-max-jug-quaj	vsy1/vsy4-ili		mt2-mt3-mt4	–	–	–
D0.5	mand	lac-fro-sqpa	pre-pal-pte-max-jug-quaj	vsy1/vsy5-ili / pub-isch		mt23-mt4	–	–	–
D1	mand		lac-fro-sqpa-pre-pal-pte-max-jug-quaj	vsy1/vsy6-ili / pub-isch		mt23-mt4	–	–	–
D1.5	mand		lac-fro-sqpa-nas-pre-pal-pte-max-jug-quaj / pasp-bas	vsy1/vsy6-ili / vth1/vth5	pub-isch	mt23-mt4	–	–	–
D2.5	mand		lac-fro-sqpa-nas-pre-pal-pte-max-jug-quaj-pasp-bas-exo-sup	vth1/vth5-vsy1/vsy12-ili	pub-isch	mt23-mt4	-	-	-
D3	mand		lac-fro-sqpa-nas-pre-pal-pte-max-jug-quaj-pasp-bas-exo-sup-mes	vce1/vce14-vth1/vth5-vsy1/vsy12-ili	pub-isch	mt23-mt4	–	–	–
D4.5	mand		lac-fro-sqpa-nas-pre-pal-pte-max-jug-quaj-pasp-bas-exo-sup-mes-lat-qua	vce1/vce14-cin1/2-vth1/vth5-cvv1/cvv5-vsy1/vsy12-csv1-ili	pub-isch	tmt	–	–	–
D6	mand		lac-fro-sqpa-nas-pre-pal-pte-max-jug-quaj-pasp-bas-exo-sup-mes-lat-qua-vce1/vce14-cin1/2-vth1/vth5-cvv1/5-vsy1/vsy12-csv1-ili		pub-isch	tmt	–	–	–
D9	mand		lac-fro-sqpa-nas-pre-pal-pte-max-jug-quaj-pasp-bas-exo-sup-mes-lat-qua-vce1/vce14-cin1/2-vth1/vth5-cvv1/cvv5-pelv1-csv1-vsy5/vsy12		pub-isch	tmt	scal-cor	–	–
D12	mand		lac-fro-sqpa-nas-pre-pal-pte-max-jug-quaj-pasp-bas-exo-sup-mes-lat-qua-vce1/vce14-cin1/cin2-vth1/vth5-cvv1/cvv5-pelv2-csv1-vsy7/vsy12-pub-isch			tmt	scal-cor-fur	–	–
D15	mand-cran1-lac-fro-sqpa-nas-pre-pal-pte-max-jug-quaj-mes-lat-qua-vce1/vce14-cin1/cin2-vth1/vth5-cvv1/cvv5-pelv3-csv1-vsy10/vsy12-pub-isch-vca1/vca7					tmt	scal-cor-fur	–	cer-bah
D18	mand-cran1-lac-fro-sqpa-nas-pre-pal-pte-max-jug-quaj-mes-ect-lat-qua-vce1/vce14-cin1/cin2-vth1/vth5-cvv1/cvv5-pelv3-csv1-vsy10/vsy12-pub-isch-vca1/vca7-fem-tbt-fib-tmt-mt1-d1p1/u-d2p1/u-d3p1/u-d4p1/u						scal-cor-fur	–	cer-bah-uro
D22	mand-cran1-cran2-maxil-pte-max-jug-quaj-qua-vce1/vce14-cin1/cin2-vth1/vth5-cvv1/cvv5-pelv4-csv1-vca1/vca5-pyg-fem-tbt-fib-tmt-mt1-d1p1/u-d2p1/u-d3p1/u-d4p1/u						scal-cor-fur-hum		pg-bar-uro-cer
A	mand-cran-maxil-arj-pte-qua-vce1/vce14-cin1/cin2-vth1/vth5-cvv1/cvv5-pelv-csv1-vca1/vca5-pyg-fem-tbt-fib-tmt-mt1-d1p1/u-d2p1/u-d3p1/u-d4p1/u-ster-scal-cor-fur-hum-rad-uln-crad-culn-cmc-pda-ppdm-pddm-pdmi								par-baur-cer-epb

Stage (S), day (D) and adult (A). For abbreviations see Table 1

Fig. 1 Anatomical network of an adult skeleton of *Myiopsitta monachus* showing the proportional size of nodes according to their connectivity degree and colored nodes according to the anatomical regions (for abbreviations of nodes see Table 1)

vertebrae 1 to 12) with the coxal bones (ilium, ischium and pubis).

In the hindlimbs, the fusion of the metatarsal II and the metatarsal III occurs at day 0.5, and then they fuse with the metatarsal IV at day 4.5 making up the tarsometatarsus. While in the forelimbs, the fusion of the alular metacarpal (II) + mayor metacarpal (III) + minor metacarpal (IV) that make up the carpometacarpus is observed in the adult.

The pygostyle is formed with the fusion of the two last caudal vertebrae at day 22.

Finally, the remaining fusions occur in the adult. These are the maxillary (jugal process) + jugal + quadratojugal bones that make up the jugal bar, the paraglosals + basihyal + urohyal bones that make up the hyoid apparatus, and

the fusion of the uncinate processes + vertebral ribs at the postcranial axial skeleton.

Network Analysis Parameters (Table 3)

The parameters measured for the whole network result from the combination of node parameters and allow comparing the networks that represent each stage of embryonic development or day after hatching during development. In addition, the simple degree of each node allows dynamic assessment of the burden rank of each bone as it grows. We have also defined an ad hoc parameter, number of dynamic skeletal assemblages, which change for each stage/age, and give a very clear description of how the ontogeny of connections proceeds.

Fig. 2 Anatomical networks of the skeleton of *Myiopsitta monachus* throughout development, from embryological stage 34 to day 22 post-hatching. The dynamic skeletal assemblages (DSAs) formation can be seen delimited for all stages/ages. The colors of the nodes follow the anatomical regions of Fig. 1
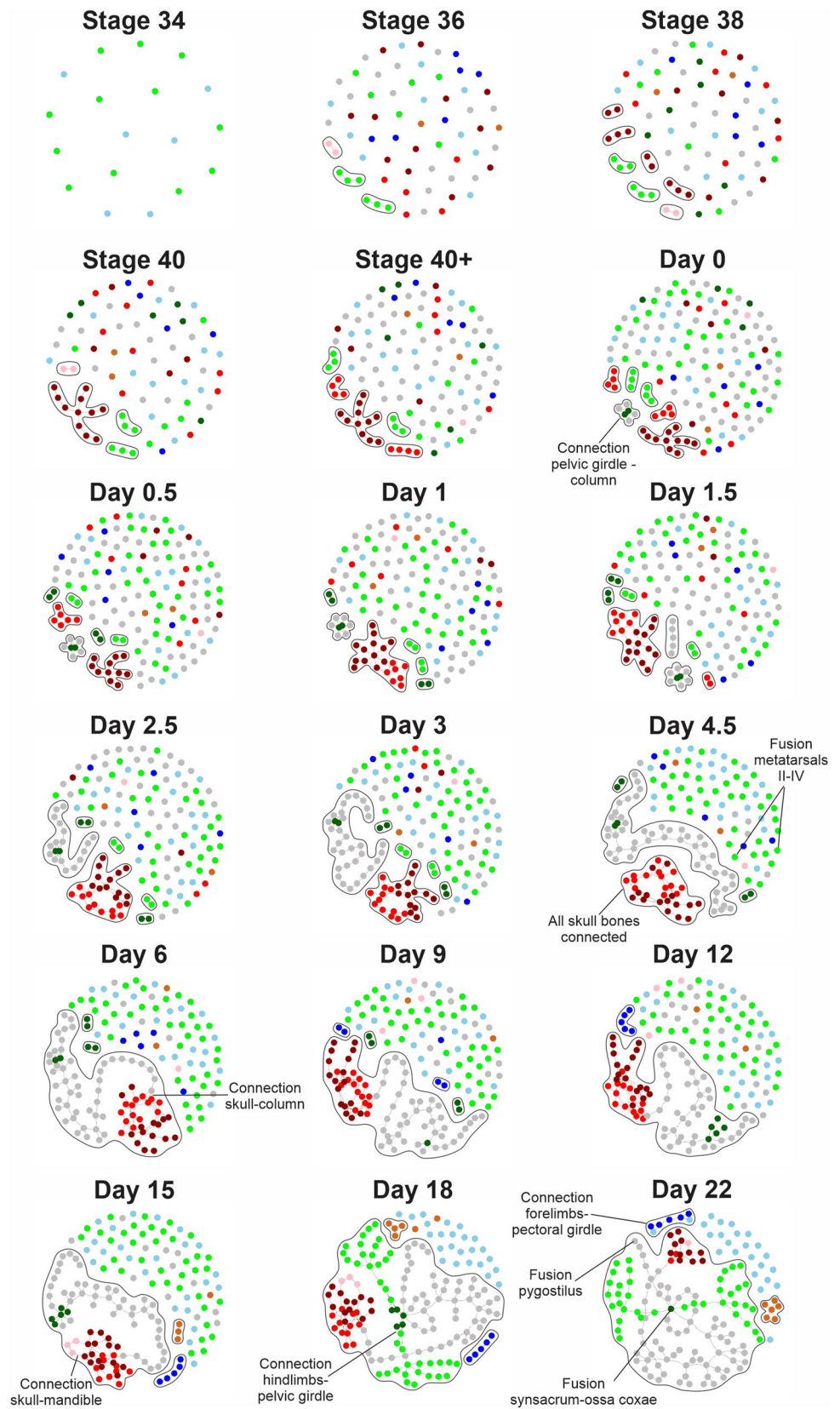
Table 3 Network analysis parameters throughout the development of *Myiopsitta monachus*

	N	K	D	L	C	H	DSAs
S34	18	0	–	–	–	–	–
S36	65	5	0.002	1.286	0	2.868	3
S38	76	11	0.004	1.267	0	1.939	7
S40	79	15	0.005	2.726	0	2.036	4
S40+	116	20	0.003	2.575	0	2.133	5
D0	144	30	0.003	2.341	0.222	2.152	6
D0.5	146	30	0.003	2.347	0	2.262	7
D1	146	38	0.004	3.086	0.076	2.213	6
D1.5	146	45	0.004	2.901	0.125	1.964	8
D2.5	150	68	0.006	3.614	0.296	1.707	6
D3	155	86	0.007	7.070	0.228	1.440	6
D4.5	153	110	0.009	6.960	0.278	1.291	4
D6	154	119	0.010	12.478	0.310	1.319	3
D9	160	109	0.009	12.426	0.200	1.369	5
D12	160	112	0.009	12.234	0.194	1.365	2
D15	161	110	0.009	12.688	0.193	1.316	3
D18	163	167	0.013	13.490	0.138	0.847	3
D22	154	153	0.013	11.427	0.119	0.799	3
A	132	169	0.020	10.665	0.129	0.613	2

Stage (S), day (D), adult (A), number of nodes (N), number of interactions (K), density of connections (D), mean shortest path length (L), mean cluster coefficient (C), heterogeneity (H), and dynamic skeletal assemblages (DSAs)

Number of Nodes (N)

The number of bones starts with a low count of 18 at stage 34, growing rapidly to 144 at hatching (day 0) and reaching a maximum of 163 at day 18 as new elements ossify. As development proceeds, bones start to fuse till the adult with a network of 132 bones.

Number of Interactions (K)

Connections among bones grow at a much slower pace than number of nodes. At stage 34 there are no connections among developing bones. By hatching (day 0) there are 30 connections, and from then on it grows steadily till reaching a maximum number of 169 connections in the adult. It is noticeable that between day 4.5 and day 15, the number of connections seems to stabilize in the range of 110 to 119; this local maximum is reached at day 6, and then K diminishes again till reaching 110. This is due to the fusion of bones and, consequently, to the reduction of nodes and modification of connections between elements. At this point a large increase in the number of connections occurs, increasing from 110 to a maximum of 169 in the adult.

Connectivity (Degree, ki) (Supplementary Material 1)

The sum of connections that a specific node has to other nodes in the network has a range between 1 and 13. The nodes that have higher k_i values throughout development are those of the skull, maxilla and palate, pelvic girdle and hindlimbs. In the adult, the values change, with the sternum being the node with the highest k_i (13).

Density of Connections (D)

All networks are very sparse; density never reaches 2% of the possible connections. This is due to the high number of isolated bones throughout development and to the fact that most bones take part in linear anatomical arrangements, such as the vertebrae and the digits. Density increases as the number of nodes also increases, reaching the maximum in the adult (almost 2%). Density values for the whole monk parakeet are very low overall.

Mean Shortest Path Length (L)

This parameter measures how close nodes are in terms of their connectivity; the lower, the more integrated. In general, bones are very close together till the first linear anatomical part (the vertebral column) starts to connect.

From then on, as the other elements in the vertebral column as well as the limbs start to connect, L increases to an average of about 12 steps.

Mean cluster coefficient (C)

This average is a measure of how tight (integrated) the network is. Basically, it measures the number of triangulations in the system. Again, figures are low because of the high number of isolated bones as well as the linear anatomical parts. At day 0.5, C drops to 0 (no triangular configurations among the bone connections) and then it climbs to 0.3 at day 6. After this maximum, there is a steady decay down to 0.12 in the adult.

Heterogeneity (H)

This is a measure of how regular the system is in terms of individual number of connections for each bone. There is a clear decrease in H from stage 38 (2.8) to the adult, where it reaches its minimum (0.61). This could be due to the high

number of bones connected to two other elements in the limbs and vertebral column.

Dynamic Skeletal Assemblages (DSAs) (Fig. 3)

The growing system is a heterogeneous combination of groupings or assemblages (i.e. connected bones) and isolated bones, whose numbers and connections change dynamically as the monk parakeet grows. Different anatomical parts connect at different times and with different rhythms; at each stage/age the number and composition of each assemblage changes dynamically, as does the number of isolated bones, as new bones appear, existing bones fuse, or new connections are established (see Table 2 and Fig. 2 for an overall picture of this process). The skeletal system reaches its maximum number of groupings (8 DSAs) at day 1.5 post-hatching; thereafter, bones start to connect to each other, diminishing the number of DSAs till reaching the adult stage. Two main large DSAs are observed in the growing system formed with nodes of the skull + maxilla + palate and nodes of the pelvic girdle + vertebral column. Throughout development, nodes are added to these two DSAs; eventually

Fig. 3 Main dynamic skeletal assemblages (DSAs) during development of the skeleton of *Myiopsitta monachus*. The colors of the nodes follow the anatomical regions of Fig. 1. For details of the nodes see Tables 1 and 2, and Supplementary Materials 1 and 2
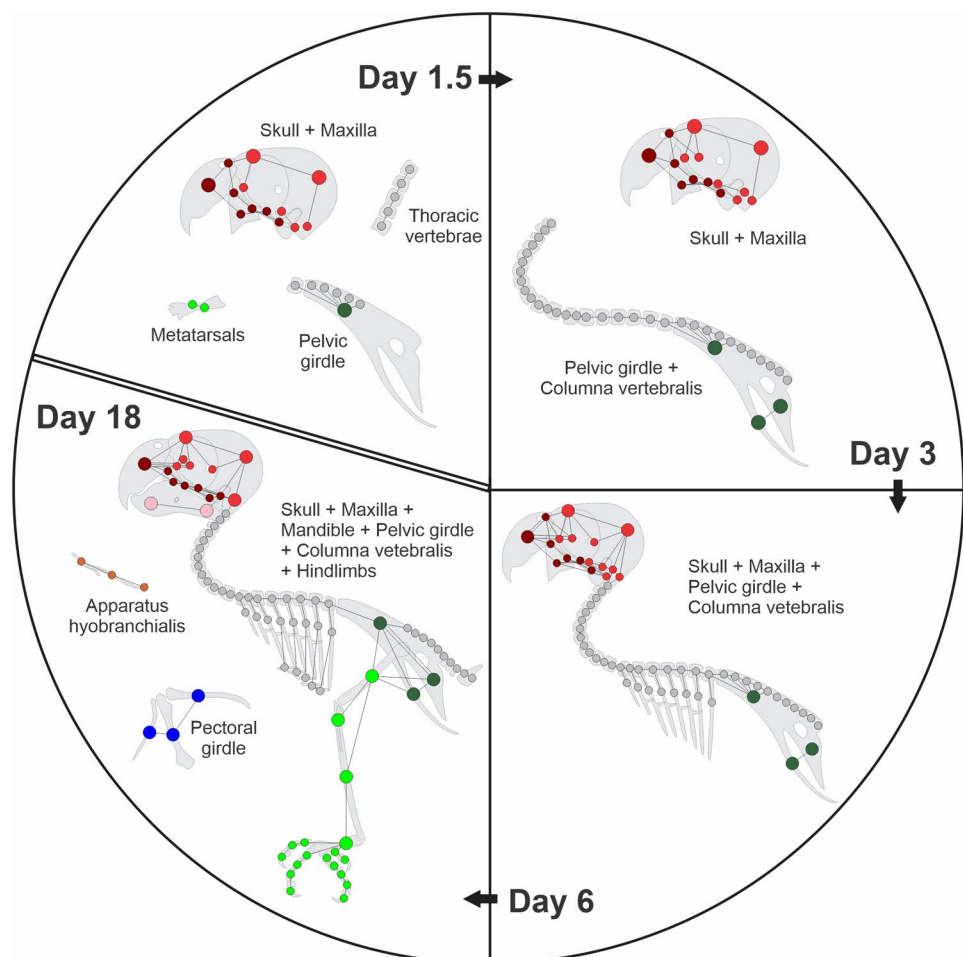
joining together to make up a large one at day 6 via the skull-cervical vertebra 1 (atlas) connection. Nodes of the pelvic girdle are all connected to each other and to this large DSA at day 12 while nodes of the hindlimbs are connected to each other and to the pelvic girdle at day 18. Nodes of the pectoral girdle (except for the sternum) connect with each other to make up a separate DSA at day 12, which connects to the large DSA in the adult along with the nodes of the forelimbs. The adult skeleton is finally composed of just two DSAs: the entire skeleton and the hyoid apparatus.

Discussion

Connectivity and Fusion Patterns During Development

Fusion of individual elements modifying several regions of the avian skeleton is one of the most striking evolutionary changes that has occurred among vertebrates and has sparked deep interest in its relationship with flight and loco-motors capabilities (Heers and Dial 2012). Although little is known about the timing at which fusions occur, several authors have pointed out that they occur after hatching (Jollie 1957; Hogg 1978, 1982; Bailleul et al. 2016; Rashid et al. 2018; Skawiński et al. 2020). In our results, through the ontogenetic development of the monk parakeet, 31 of a total of 163 bones (19%) lose independence due to fusions, the majority in the skull between day 22 after hatching and adult. The logical consequence of these fusions is the decrease in the number of nodes within the skeleton network, that is, bones or sets of fused bones independent of others. Fusions are inevitably preceded by the connection (physical junctions) between the elements involved. A recent study of postnatal ontogenetic changes and modularity in the skulls of birds using AnNA also show that juveniles have a greater number of bones and connections than adults; this translates into less integrated skulls and in an integration increase during development due to fusions (Plateau and Foth 2020). In monk parakeets, before hatching, approximately 71% of the elements are ossified (Carril and Tambussi 2017) and, as shown in our result, only 20 connections were established, this is almost 12% of all possible connections (169 in the adult) between the elements. Through development the connections increase with a staggered rhythm and a major peak at day 18.

Certainly, understanding the construction of the avian skull is important in interpreting evolutionary drivers of its architecture. Due to the fused nature of the avian skull, limits between the bones in the adult are not well defined. At hatching, the skull is a miniature of the adult skull, but fusions are established much later. In the bibliography we find that at

hatching, the precocial chicken *Gallus gallus* have 27 connections (Hogg 1978), while the monk parakeet has a total of 36. The first skull bones to fuse together in the monk parakeet are the squamosals and the parietals at day 0.5, followed by the fusion between the occipital and the parasphenoidal bones at day 15. The remaining skull bones complete their fusion between day 22 and the adult. Synostosis in precocial birds, such as the chicken, begins with the fusion of the basioccipital and the exoccipitals on day 39, continues in the occipital region in chicks of 75 days, and ends at the level of the frontals at day 100 (Jollie 1957; Hogg 1978). This indicates that cranial fusions occur earlier in the monk parakeet than in the chicken. We must note, however, that the data from the literature regarding the moments of fusion in chickens is dissimilar and, even in the same work, the information is contradictory (Hogg 1982). The cause may lie in the variation in how data is captured and in the uncertainty of the chicks' ages. For example, basioccipital-exoccipitals contact occurs in some individuals at 14 days and in others at 49 days. Perhaps for this reason, Hogg (1978) calculates the "mean fusion time" between bones. We can realize that, although timing is not the same, fusions of skull bones occur after hatching in the altricial monk parakeet and other birds (Hogg 1978; Plateau and Foth 2020). Similarly, postcranial skeleton fusions occur after hatching in both the monk parakeet and the chicken (Hogg 1982; Rashid et al. 2018).

Unlike skeletogenesis, which occurs antero-posteriorly (Carril and Tambussi 2017), the connection of the vertebrae to form the vertebral column do not follow such a linear pattern. However, certain bi-directional pattern can be discerned, with the synsacral vertebrae as the first ones to connect with the ilia, and the thoracic vertebrae as the first ones to connect with each other; from there, the vertebral column connections follow posteriorly (first the synsacral and then the caudal vertebrae) and anteriorly (the cervical vertebrae). A possible hypothesis to explain this pattern concerns the rate of growth of each vertebra; a faster growth would imply an earlier connection (Esteve-Altava and Rasskin-Gutman 2014a). Thus, we can speculate that, since all vertebrae are present at the onset of connections in the column (except the caudal vertebrae) a postero-anterior gradient of growth-rate is established from the thoracic region.

Pelvic girdle and hindlimbs connections begin and end before those of the pectoral girdle and the forelimbs. These connectivity patterns match well with the known skeletogenesis process of the monk parakeet: the ossification onset of the hindlimbs bones occurs before those of the forelimbs (Carril and Tambussi 2017). All possible connections between the bones of the vertebral column, pelvic girdle and hindlimbs are established in the monk parakeet prior to the active walking movements of the nestlings inside the nest (at 18th day post-hatching, Aramburú 1997). Also, the connection and posterior fusion of the last caudal vertebrae

making up the pygostyle is a post-hatching event in the monk parakeet. The formation of the pygostyle determines the flight capacity and therefore limits the nestlings from leaving the nest. For the monk parakeet this happens around the 40th day post-hatching (Aramburú 1997). From these observations, we can infer that the connection among the elements of a certain complex is a necessary condition for its functionality. This presumption allows us to predict that the connection between the elements of the forelimb must occur between the 22nd and 44nd days post-hatching.

The Network Ontogeny and the Avian Body Plan

The other question that guided this research was the attempt to understand which connections and fusions of bones occurring during development could be associated with morphological changes linked to the avian body plan. The degree of connectivity for each bone is a proxy for burden rank (Rasskin-Gutman and Esteve-Altava 2014), and thus potentially indicates the importance of bones from an Evo-Devo point of view, an aspect that can be seen as "morphological evolvability". The burden rank of an anatomical element is a measure of developmental and functional constraint: the more connected an element is, the more constrained by its developmental and functional dependencies (Riedl 1978). As a consequence of these constraints, these highly connected bones are expected to show a high degree of morphological conservatism. Fusion with other bones could also be a direct result of high connectivity values (Rasskin-Gutman and Esteve-Altava 2018). One point that emerges from this assumption is that elements that fuse during ontogeny and characterize the avian body plan show a high degree of connectivity (k_i). In our networks, higher connectivity values are exhibited by the premaxillar and the parasphenoidal bones. Similarly high connectivity values are found in most of the skull bones (e.g. frontal, squamosal, parietal, mesethmoidal, supraoccipital). After hatching, the ilium (day 0) and the pelvis (from day 6 on) exhibit one of the highest k_i values. Also, the tarsometatarsus (metatarsals II-IV already fused) has high k_i values from day 18 on, but in this case, high k_i values occur by connection to the digits and not by further fusion.

The network assemblages highlight a characteristic Evo-Devo pattern encapsulated in Karl Ernst von Baer's first law (one of the four well-known laws of development) which, in a cladistic reformulation, assumes that characters more widely distributed within a higher hierarchy clade manifest earlier in ontogeny than less widely distributed characters (Wallace 1997). Undoubtedly, this developmental law has profound implications for the evolution of animal lineages; in the case of the avian lineage, most of the features that assembled the modern bird body plan throughout a hierarchically-diversified process pertain to the skeleton (Cau

2018). In fact, 99% of the evolutionary events involve the skeleton, and the remaining 1% the integumentary system (Cau 2018). These skeletal features, which are concentrated in the skull, pelvis and limb bones, are those that would be expected to be more conserved. Indeed, the pattern we see with their network assemblages is consistent with high connectivity values (k_i) from early stages of development; since higher connectivity degree (k_i) implies higher burden rank, and thus higher morphological conservatism.

As previously mentioned, the simplification of the skeleton that characterizes the avian body plan is associated with the fusion of the skull, pelvis, limbs bones and pygostyle. For example, pygostyle formation is a key milestone in the evolution of birds, dating from around 131 Ma (Chiappe and Witmer 2002; Chatterjee 2015). Shorter tails are more aerodynamic and, in consequence, linked to flight capacity and the diversification of modern birds (Makovicky and Zanno 2011). Because of that, several anatomists have concentrated their research on elucidating when and how the pygostyle forms. Our network results agree with the general pattern found where the pygostyle formation occurs as a post-hatching event in altricial species (Starck 1993; Maxwell 2008; Carril and Tambussi 2017). However, it has been observed that there is a notable variation in the timing of pygostyle formation, even when dealing with the same species (e.g. chicken *Gallus gallus*; Hogg 1982; Skawiński et al. 2020). Other reports indicate that in the chicken, pygostyle fusion has not ended in 7/8 week old chicks since the medullary canal and intervertebral discs are still present; these differences are probably due to the dissimilar criteria used to define the pygostyle and to the different techniques used to study its formation (Rashid et al. 2018).

Finally, the network descriptors analyzed in this study places the developmental focus on the moment of appearance, connection, and fusion of skeletal parts. Thus, the developing monk parakeet is seen as a system of elements that group into coherent networks, that we call the "dynamic skeletal assemblages" (DSAs), which change by means of bone fusions and new connections with isolated elements, as well as by connections to other DSAs (Table 2, Figs. 2 and 3). After hatching, there is a predominance of two main DSAs in terms of the number of elements; one made up of elements of the pelvic girdle, the hindlimbs and the vertebral column, and the other made up of skull elements. These two major DSAs become connected to each other at day 6, behaving as connectivity attractors to other bones, until the adult is finally fully formed as a system of two networks, the hyoid apparatus plus the rest of the skeleton. These two DSAs may have been part of the first manifestations of the neornithine body plan, a plan that dates back at least 70 million years (Clarke et al. 2005). It would be interesting to analyze what happens in other birds with different types of development and belonging to different groups throughout

the entire phylogeny. Regardless of the developmental type and the phylogenetic relationship of all neornithine, we predict that the bones with higher connectivity degree (ki) and the DSAs described here are conserved since they define the avian body plan.

Conclusions

The development of the monk parakeet can provide new insights into how the connections of the elements of the skeleton form in a highly altricial bird. We hypothesize that connections of the girdles and limbs could be linked to the altriciality due to requirements for active movement in the use of the hindlimbs inside the nest, but not the need to use forelimbs to fly until much later. The network connection sequence corresponding with life history, could have important evolutionary implications, but must be tested on other birds with different types of development within the precocial-altricial spectrum.

Also, we hypothesize that there is consistency between the connectivity pattern and the avian body plan. The bones most centrally involved in the construction of the avian body plan have the highest connectivity values of the entire system and are included in the main DSAs that change dynamically and behave as connectivity attractors as bones condense, fuse or connect to each other during ontogeny.

Because selection can act on phenotypes during development, a modification that occurs in a taxon could have a high impact for evolvability; hence the importance of understanding in detail how a structure is built. The study of connections and fusions of individual bones during ontogeny provides valuable information on how the adult skeleton is formed. This information is morphological, but not centered on shape and size; rather, it shifts the focus on an entirely new morphologically perspective, that of connectivity among related anatomical parts, restructuring the questions in terms of growing parts that interact within a complex system, and exposing new local and global structural properties of the developing organism.

Author Contributions JC: study conception and design-equal, material preparation and data collection-lead, writing original draft-equal, writing-review & editing-equal. CPT: study conception and design-equal, writing original draft-equal, writing-review & editing-equal. DR-G: study conception and design-supporting, formal data analysis-lead, writing-review & editing-equal.

Compliance with Ethical Standards

Conflict of interest The authors declare that they have no conflict of interest.

Ethical Approval The authors declare that the materials used were obtained complying with the current laws of the country in which they were performed (Argentina).

Informed Consent All authors agree to participate in the manuscript and obtain consent from the responsible authorities at the institute where the work has been carried out.

References

Aramburú, R. M. (1997). Descripción y desarrollo del pichón de la cotorra *Myiopsitta monachus monachus* (Aves: Psittacidae) en una población silvestre de Argentina. *Revista Chilena de Historia Natural, 70,* 53–58.

Bailleul, A. M., Scannella, J. B., Horner, J. R., & Evans, D. C. (2016). Fusion patterns in the skulls of modern archosaurs reveal that sutures are ambiguous maturity indicators for the Dinosauria. *PLoS ONE, 11,* e0147687.

Baumel, J. J., & Witmer, L. M. (1993). Osteologia. In J. J. Baumel, A. S. King, J. E. Breazile, H. E. Evans, & J. C. Vannden Berge (Eds.), *Handbook of avian anatomy: Nomina anatomica avium.* Nuttall ornithological club, no. 23 (2nd Ed.) (pp. 45–132). Cambridge, MA: Museum of Comparative Zoology, Harvard University.

Canavelli, S. B., Swisher, M. E., & Branch, L. C. (2013). Factors related to farmers' preferences to decrease monk parakeet damage to crops. *Human Dimensions of Wildlife, 18,* 124–137.

Carril, J., & Tambussi, C. P. (2015). Development of the superaltricial monk parakeet (Aves, Psittaciformes): Embryo staging, growth, and heterochronies. *The Anatomical Record, 298,* 1836–1847.

Carril, J., & Tambussi, C. P. (2017). Skeletogenesis of *Myiopsitta monachus* (Psittaciformes) and sequence heterochronies in Aves. *Evolution & Development, 19,* 17–28.

Cau, A. (2018). The assembly of the avian body plan: A 160-million-year long process. *Bollettino della Società Paleontologica Italiana, 57,* 1–25.

Chatterjee, S. (2015). *The rise of birds: 225 million years of evolution* (2nd ed.). Baltimore: Johns Hopkins University Press.

Chiappe, L. M., & Witmer, L. M. (2002). *Mesozoic birds: Above the heads of dinosaurs.* Berkeley, CA: University of California Press.

Clarke, J. A., Tambussi, C. P., Noriega, J. I., Erickson, G. M., & Ketcham, R. A. (2005). Definitive fossil evidence for the extant avian radiation in the Cretaceous. *Nature, 433,* 305–308.

Collar, N. J. (1997). Family Psittacidae (parrots). In J. Del Hoyo, A. Elliott, & J. Sargatal (Eds.), *Handbook of the birds of the world: sandgrouse to cuckoos* (Vol. 4, pp. 280–477). Barcelona: Lynx Editions.

Csardi, G., & Nepusz, T. (2006). The igraph software package for complex network research. *InterJournal Complex Systems, 1695,* 1–9.

Dingerkus, G., & Uhler, D. (1977). Enzyme clearing of alcian blue stained whole small vertebrates for demostation of cartilage. *Stain Technology, 52,* 229–232.

Esteve-Altava, B., Botella, H., Marugán-Lobón, J., & Rasskin-Gutman, D. (2013). Structural constraints in the evolution of the skull: Williston's law revisited. *Evolutionary Biology, 40,* 209–219.

Esteve-Altava, B., Diogo, R., Smith, C., Boughner, J. C., & Rasskin-Gutman, D. (2015). Anatomical networks reveal the musculoskeletal modularity of the human head. *Scientific Reports, 5,* 8298.

Esteve-Altava, B., Marugán-Lobón, J., Botella, H., Bastir, M., & Rasskin-Gutman, D. (2013). Grist for Riedl's mill: A network model perspective on the integration and modularity of the human skull. *Journal of Experimental Zoology Part B: Molecular and Developmental Evolution, 320,* 489–500.

Esteve-Altava, B., Marugán-Lobón, J., Botella, H., & Rasskin-Gutman, D. (2014). Random loss and selective fusion of bones originate morphological complexity trends in tetrapod skull networks. *Evolutionary Biology, 41,* 52–61.

Esteve-Altava, B., & Rasskin-Gutman, D. (2014a). Beyond the functional matrix hypothesis: A network null model of human skull growth for the formation of bone articulations. *Journal of Anatomy, 225,* 306–316.

Esteve-Altava, B., & Rasskin-Gutman, D. (2014b). Theoretical morphology of tetrapod skull networks. *Comptes Rendus Palevol, 13,* 41–50.

Esteve-Altava, B., & Rasskin-Gutman, D. (2015). Evo-Devo insights from pathological networks: Exploring craniosynostosis as a developmental mechanism for modularity and complexity in the human skull. *Journal of Anthropological Sciences, 93,* 103–117.

Esteve-Altava, B., & Rasskin-Gutman, D. (2018). Anatomical network analysis in Evo-Devo. In L. Nuño de la Rosa & G. B. Müller (Eds.), *Evolutionary developmental biology* (pp. 1–19). New York: Springer.

Esteve-Altava, B., Vallès Català, T., Guimerà, R., Sales-Pardo, M., & Rasskin-Gutman, D. (2017). Bone fusion in normal and pathological development is constrained by the network architecture of the human skull. *Scientific Reports, 7,* 3376.

Heers, A. M., & Dial, K. P. (2012). From extant to extinct: Locomotor ontogeny and the evolution of avian flight. *Trends in Ecology and Evolution, 27,* 296–305.

Hogg, D. A. (1978). The articulations of the neurocranium in the postnatal skeleton of the domestic fowl (*Gallus gallus domesticus*). *Journal of Anatomy, 127,* 53–63.

Hogg, D. A. (1982). Fusions occurring in the postcranial skeleton of the domestic fowl. *Journal of Anatomy, 135,* 501–512.

Jollie, M. T. (1957). The head skeleton of the chicken and remarks on the anatomy of this region in other birds. *Journal of Morphology, 100,* 389–436.

Lee, M. S. Y., Cau, A., Naish, D., & Dyke, G. J. (2014). Morphological clocks in palaeontology, and a mid-Cretaceous origin of crown Aves. *Systematic Biology, 63,* 442–449.

Makovicky, P. J., & Zanno, L. E. (2011). Theropod diversity and the refinement of avian characteristics. In D. Gareth & G. Kaiser (Eds.), *Living dinosaurs: The evolutionary history of modern birds* (1st ed., pp. 9–29). New York: Wiley.

Maxwell, E. E. (2008). Comparative embryonic development of the skeleton of the domestic turkey *Meleagris gallopavo* and other galliform birds. *Zoology, 111,* 242–257.

Navarro-Díaz, D., Esteve-Altava, B., & Rasskin-Gutman, D. (2019). Disconnecting bones within the jaw-otic network modules underlies mammalian middle ear evolution. *Journal of Anatomy, 235,* 15–33.

Plateau, O., & Foth, C. (2020). Birds have peramorphic skulls, too: Anatomical network analyses reveal oppositional heterochronies in avian skull evolution. *Communications Biology, 3,* 1–12.

Prum, R. O., Berv, J. S., Dornburg, A., Field, D. J., Townsend, J. P., Moriarty Lemmon, E., & Lemmon, A. R. (2015). A comprehensive phylogeny of birds (Aves) using targeted next-generation DNA sequencing. *Nature, 526,* 569–573.

R Development Core Team. (2019). *R: A language and environment for statistical computing*. Vienna, Austria: R Foundation for Statistical Computing.

Rashid, D. J., Surya, K., Chiappe, L. M., Carroll, N., Garrett, K. L., Varghese, B., et al. (2018). Avian tail ontogeny, pygostyle formation, and interpretation of juvenile Mesozoic specimens. *Scientific Reports, 8,* 1–12.

Rasskin-Gutman, D., & Esteve-Altava, B. (2014). Connecting the dots: Anatomical network analysis in morphological EvoDevo. *Biological Theory, 9,* 178–193.

Rasskin-Gutman, D., & Esteve-Altava, B. (2018). Concept of burden in Evo-Devo. In L. Nuño de la Rosa & G. B. Müller (Eds.), *Evolutionary developmental biology* (pp. 1–11). New York: Springer.

Ricklefs, R. E., & Starck, J. M. (1998). Embryonic growth and development. In R. E. Ricklefs & J. M. Starck (Eds.), *Avian growth and development. Evolution within the altricial precocial spectrum* (pp. 31–58). New York: Oxford University Press.

Riedl, R. (1978). *Order in living organisms: A systems analysis of evolution*. New York: Wiley.

Schoch, R. R. (2010). Riedl's burden and the body plan: Selection, constraint, and deep time. *Journal of Experimental Zoology, 314B,* 1–10.

Skawiński, T., Borczyk, B., & Hałupka, L. (2020). Postnatal ossification sequences in *Acrocephalus scirpaceus* and *Chroicocephalus ridibundus* (Aves: Neognathae): The precocial–altricial spectrum and evolution of compound bones in birds. *Journal of Anatomy, August,* 1–16.

Starck, J. M. (1993). Evolution of avian ontogenies. In D. M. Powers (Ed.), *Current ornithology* (pp. 275–366). New York: Plenum Press.

Wallace, A. (1997). *The origin of animal body plans: A study in evolutionary developmental biology*. Cambridge: Cambridge University Press.